doi:10.3788/gzxb20184708.0823001

超小型带宽可调谐微环谐振腔

董文[1],邹雨[2],杜颖[2],乐孜纯[2]
(1 浙江工业大学 环境学院,杭州 310014)
(2 浙江工业大学 理学院,杭州 310023)

摘 要:基于狭缝波导和热光学调制的耦合特性,提出一种尺寸为 15 μm×20 μm 的绝缘硅基底的超小型微环谐振器,该器件可通过调节加热器功率调节其带宽.用时域有限差分法模拟其可调谐特性,结果表明,当加热器功率从 0 mW 增加至 0.742 mW 时,1550 nm 入射光的 TE 模式在 1 900 nm 波长下的带宽可调范围为 2.5 nm,TM 模式在 1 543 nm 波长处的带宽可调范围为 3.1 nm.该器件尺寸小、驱动功率低、可调谐带宽范围大,适用于动态集成光信号处理,如重构滤波和布线等.

关键词:集成光学;狭缝波导;时域有限差分法;微环谐振腔;热光调制
中图分类号:O439 **文献标识码**:A **文章编号**:1004-4213(2018)08-0823001-7

Ultra-compact Bandwidth-tunable Microring Resonator

DONG Wen[1], ZOU Yu[2], DU Ying[2], LE Zi-chun[2]
(1 *College of Environment, Zhejiang University of Technology, Hangzhou* 310014, *China*)
(2 *College of Sciences, Zhejiang University of Technology, Hangzhou* 310023, *China*)

Abstract: Based on the coupling characteristics of slot waveguides and the thermo-optical modulation, an ultra-compact microring resonator on silicon-on-insulator with the size of 15 μm×20 μm is proposed, whose bandwidth can be tuned by adjusting the heater power. The tunability characteristic is simulated through finite difference time domain method, the result demonstrates when the wavelength of incident light is 1 550 nm, its adjustable bandwidth range is 2.5 nm at 1 900 nm wavelength for TE mode and 3.1 nm at 1 543 nm wavelength for TM mode by applying the heater power from 0 mW to 0.742 mW. The proposed device with small size, low driving power and wide tunable range of bandwidth is very promising for dynamic integrated optical signal processing such as reconfigurable filtering and routing.

Key words: Intergrated optics; Microring resonator; Finite difference time domain; Slot waveguides; Thermo-optical modulation
OCIS Codes: 230.5750; 130.3120; 130.7408; 070.5753

0 Introduction

The high-index-contrast in Silicon-On-Insulator (SOI) waveguides allows small bending radius with low propagation losses, which leads to compact Microring Resonator (MRR) and high density integration of micro-photonic devices. MRR is regarded as a versatile component in a wide range of applications such as modulator[1], wavelength division multiplexing filter[2], wavelength converter[3] and switch[4], etc. The tunable bandwidth is the first priority for the devices used in dynamic networks, thus MRR with a tunable

Foundation item: The National Natural Science Foundation of China (No. 61172081) and the Natural Science Foundation of Zhejiang Province, China (No. LZ13F010001)
First author: DONG Wen (1965—), male, professor, M.S. degree, mainly focuses on photoelectric functional materials. Email: dongwen@zjut.edu.cn
Supervisor: LE Zi-chun(1965—), female, professor, Ph.D. degree, mainly focuses on optical communication and micro-nano photonics devices. Email: lzc@zjut.edu.cn
Received: Mar.14, 2018; **Accepted**: May.10, 2018

bandwidth will be widely used in communications network. For example, an add-drop filter could provide an adaptive control with the ability to tune bandwidth for different channels within one resonance in real time in response to a reconfigurable channel selector for Wavelength Division Multiplexing (WDM) systems[5]. Several approaches have been proposed to obtain the tunable bandwidth. For instance, a bandwidth-tunable filter has been demonstrated by Micro-Electro-Mechanical System (MEMS) actuated microdisk resonator[6], but a high actuation voltage of nearly 40 V is needed. In another example, the bandwidth-tunable MRR has been demonstrated using silicon microrings in a Mach-Zehnder Interferometer (MZI) with thermal tuning[7], but the structure is relatively complex and is difficult to control due to the introduction of MZI. A compact microring resonator (radius of 10 μm) on SOI platform with tunable bandwidth from 0.1 nm to 0.7 nm was proposed using interferometric couplers and thermal tuning[8]. An optical filter with flat-top spectral response and tunable bandwidth based on a single reflective-type MRR was proposed[9].

In this work, an ultra-compact bandwidth-tunable MRR on SOI by combining a slot waveguide[10] with thermo-optical tuning effect was demonstrated. By applying different heater powers, the refractive index difference in the coupling region is tuned, and the energy in the gap between the straight waveguide and the microring is changed as a result. The Finite Difference Time Domain (FDTD) was adopted to modulation for TE and TM mode, respectively.

1 Structure design and analysis

The schematic diagram of the bandwidth-tunable MRR is shown in Fig.1. The gap between straight and ring waveguides is expressed as Δ, and the radius of the microring resonator is R (measured from the center of microring to the central-line of ring waveguide). The close-up cross-sectional (C-C) diagram of the waveguide is shown in Fig.1(b). A and B represent straight and ring waveguide, respectively. The width a and height b of A and B waveguide are designed to be 0.3 μm and R is 5 μm, which is shown in Fig. 1(a), and Δ is 0.05 μm. A 1 μm thickness (t_{SiO_2}) buffer layer of SiO_2 is used to form the upper cladding of the waveguides for optical isolation between the thermal element and the surface defects created during facet polishing. A heater layer with 0.1 μm thickness, 4 μm width (w) and 1 μm length (L) is deposited on the top of SiO_2 for thermal-optical tuning in the coupling regions. The structure and size of coupling regions for drop and through ports in the bandwidth-tunable MRR is an identical design in order to obtain a minimum insertion loss at the resonance wavelength.

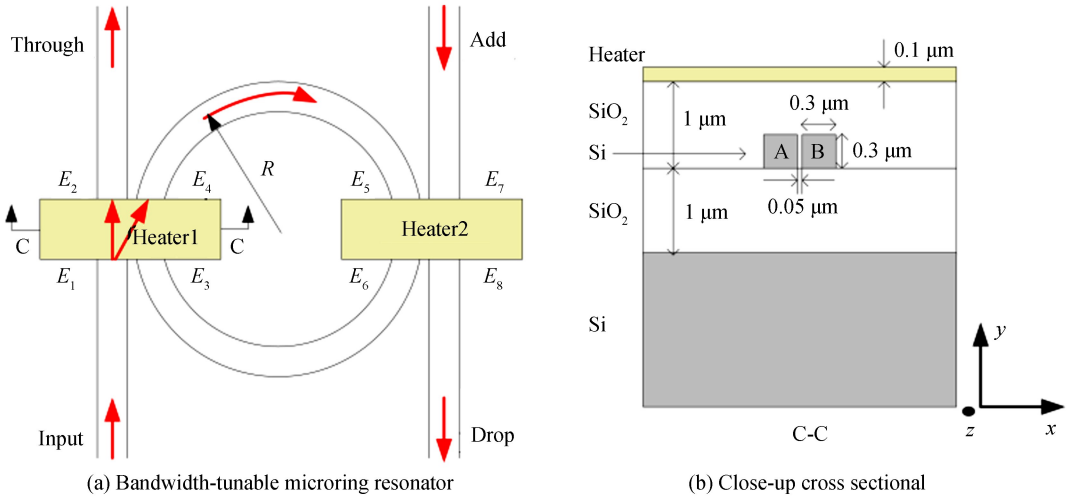

(a) Bandwidth-tunable microring resonator (b) Close-up cross sectional

Fig.1 Schematic diagram of the bandwidth-tunable microring resonator and its close-up cross sectional

The interactions in the coupling regions can be written using the followingmatrices[11]

$$\begin{bmatrix} E_4 \\ E_2 \end{bmatrix} = \begin{bmatrix} t & -\mathrm{j}\kappa \\ -\mathrm{j}\kappa & t \end{bmatrix} \begin{bmatrix} E_3 \\ E_1 \end{bmatrix} \mathrm{e}^{-\mathrm{j}\Delta\theta} \tag{1}$$

$$\begin{bmatrix} E_8 \\ E_6 \end{bmatrix} = \begin{bmatrix} t & -\mathrm{j}\kappa \\ -\mathrm{j}\kappa & t \end{bmatrix} \begin{bmatrix} E_7 \\ E_5 \end{bmatrix} \mathrm{e}^{-\mathrm{j}\Delta\theta} \tag{2}$$

where E_1, E_3, E_5, E_7 and E_2, E_4, E_6, E_8, are the input and output electric fields in the coupling regions, respectively. t and k are the self- and cross-coupling coefficients that described the coupling intensity. $\Delta\theta = 2\pi L\Delta n_{\text{eff}}/\lambda$, where L, λ are the length of the heater of one port and the resonance wavelength, respectively, Δn_{eff} is the difference of the effective index of silicon material due to the thermo-optical effect. E_5 and E_3 also can be expressed as $E_5 = \mathrm{e}^{-(\gamma+\mathrm{j}\beta)(\pi R-2L)}E_4$ and $E_3 = \mathrm{e}^{-(\gamma+\mathrm{j}\beta)(\pi R-2L)}E_6$, where β and γ stand for the propagation constant and the amplitude loss coefficient in the ring waveguide, respectively. If only a wave in the bandwidth-tunable MRR propagates clockwise and there is no input signal in the add port, then $E_6 = 0$. The spectral response at the through port therefore can be expressed as follow

$$|T|^2 = \left|\frac{E_2}{E_1}\right|^2 = \frac{t^2\left\{1+(\kappa^2+\mathrm{t}^2)^2\cdot\alpha^2-2\alpha(\kappa^2+\mathrm{t}^2)\cos\frac{4\pi}{\lambda}[n_{\text{eff}}(\pi R-2L)+L\Delta n_{\text{eff}}]\right\}}{1-2\alpha t^2\cos\frac{4\pi}{\lambda}[n_{\text{eff}}(\pi R-2L)+L\Delta n_{\text{eff}}]+\alpha^2 t^4} \tag{3}$$

The spectral response at the drop port can be expressed as follow

$$|D|^2 = \left|\frac{E_8}{E_1}\right| = \frac{\kappa^4\alpha}{1-2\alpha t^2\cos\frac{4\pi}{\lambda}[n_{\text{eff}}(\pi R-2L)+L\Delta n_{\text{eff}}]+\alpha^2 t^4} \tag{4}$$

where $\alpha = \exp[-2\gamma(\pi R-2L)] \approx \exp(-\gamma 2\pi R)$ is entitled as the inner circulation factor. In Fig. 2, the electric filed amplitude profile in the coupling region is shown by using FDTD simulation. The transmission is enhanced on the gap region between straight and ring waveguide due to the coupling effect. The initial refractive index difference Δn between core layer ($n_{\text{Si}} = 3.48$) and cladding layer ($n_{\text{SiO}_2} = 1.46$) is 2.02.

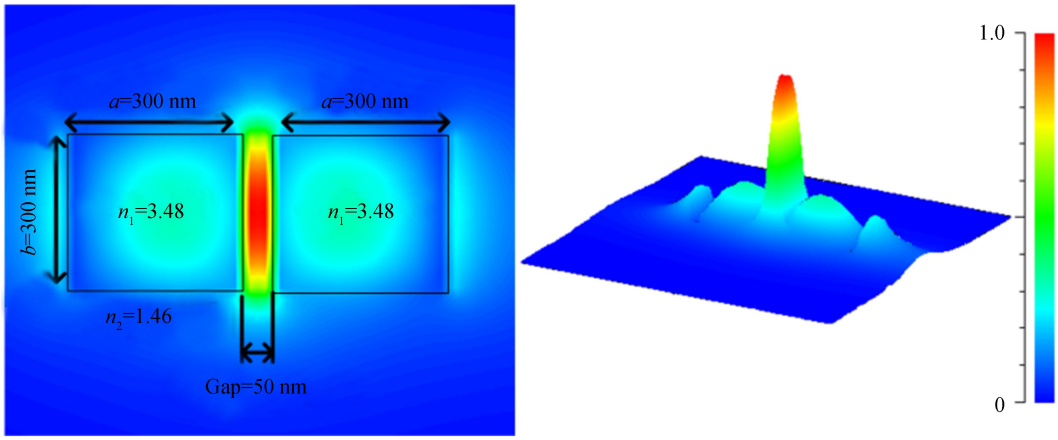

Fig.2 Contour and three-dimensional surface plot of the electric field amplitude

The bandwidth of the MRR ($\Delta\lambda$) is defined as the full width at half maximum of the resonant wavelength. In order to obtain the maximum $\Delta\lambda$, the Free Spectrum Range (FSR) is calculated firstly, which can be expressed by Eq. (5) according to resonance condition.

$$(2\pi R-2L)n_{\text{eff}}+2Ln_t = m\lambda \tag{5}$$

The FSR can be expressed as follow

$$\text{FSR} = \frac{\lambda^2 n_{\text{eff}}}{(2\pi R n_{\text{eff}}+2L\Delta n_{\text{eff}})n_g+2L\left(n_t\frac{\mathrm{d}n_{\text{eff}}}{\mathrm{d}\lambda}-n_{\text{eff}}\frac{\mathrm{d}n_t}{\mathrm{d}\lambda}\right)} \tag{6}$$

where n_t is the effective refractive index of silicon after thermo-optical modulation, and n_{eff} is the refractive index of silicon before thermo-optical modulator. $n_t\frac{\mathrm{d}n_{\text{eff}}}{\mathrm{d}\lambda}-n_{\text{eff}}\frac{\mathrm{d}n_t}{\mathrm{d}\lambda}$ can be approximately considered as zero, and n_g is the group refractive index of silicon. FSR is can also be expressed as

$$\text{FSR} = \frac{\lambda^2 n_{\text{eff}}}{(2\pi R n_{\text{eff}}+2L\Delta n_{\text{eff}})n_g} \tag{7}$$

The expression of finesse is shown as[12]

$$F=\frac{\mathrm{FSR}}{\Delta\lambda}=\frac{\pi\sqrt{\alpha t^2}}{1-\alpha t^2} \tag{8}$$

So the bandwidth of the ring resonator can be inferred from Eqs.(7) and(8)

$$\Delta\lambda=\frac{\lambda^2 n_{\mathrm{eff}}(1-\alpha t^2)}{2\pi n_{\mathrm{g}}\sqrt{\alpha t^2}\,(\pi R n_{\mathrm{eff}}+L\Delta n_{\mathrm{eff}})} \tag{9}$$

Due to the small gap of 0.05 μm between the straight waveguide and the microring, the slot waveguide effect appears. The energy distribution in the coupling region will change and there is more energy is constrained in the low-index gap between the straight waveguide and the microring, which is shown in Fig.2. Due to the slot waveguide effect, the usual assumption $\kappa^2+t^2=1$ is no longer valid, actually, $\kappa^2+t^2<1$. Therefore an energy factor K is defined, in which $K^2=\kappa^2+e_{\mathrm{gap}}^2$. It is clear that $K^2+t^2=1$ according to energy conservation, and e_{gap} is related to the energy constrained in the gap. $K^2+t^2=1$ is substituted in Eqs.(3), (4) and (9)

$$|T|^2=\left|\frac{E_2}{E_1}\right|^2=\frac{(1-K^2)\left\{1+(1-e_{\mathrm{gap}}^2)^2\cdot\alpha^2-2\alpha(1-e_{\mathrm{gap}}^2)\cos\frac{4\pi}{\lambda}[n_{\mathrm{eff}}(\pi R-2L)+L\Delta n_{\mathrm{eff}}]\right\}}{1-2\alpha(1-K^2)\cos\frac{4\pi}{\lambda}[n_{\mathrm{eff}}(\pi R-2L)+L\Delta n_{\mathrm{eff}}]+\alpha^2\,(1-K^2)^2} \tag{10}$$

$$|D|^2=\left|\frac{E_8}{E_1}\right|=\frac{\kappa^4\alpha}{1-2\alpha(1-K^2)\cos\frac{4\pi}{\lambda}[n_{\mathrm{eff}}(\pi R-2L)+L\Delta n_{\mathrm{eff}}]+\alpha^2\,(1-K^2)^2} \tag{11}$$

$$\Delta\lambda=\frac{\lambda^2 n_{\mathrm{eff}}[1-\alpha(1-K^2)]}{2\pi n_{\mathrm{g}}\sqrt{\alpha(1-K^2)}\,(\pi R n_{\mathrm{eff}}+L\Delta n_{\mathrm{eff}})} \tag{12}$$

From Eq. (9), we can see the bandwidth-tunable MRR can be achieved by changing the refractive index of n_{eff} in the coupling region. However, the tunable range of bandwidth will be very small because of the small inductive change of n_{eff}. By comparison Eq. (12) with Eq. (9), the change of the energy in the gap (related to K) due to the slot phenomenon produces the bandwidth-tunable of MRR, which can be attained by changing n of Si due to the thermo-optical effect in the coupling region. Therefore, a much larger tunable range of band width can be achieved by the combination of slot waveguides in the coupling region with thermo-optical tuning.

2 Simulations results and discussion

By using FDTD method, the coupling effect between the straight waveguide and microring waveguide is studied by injecting a continuous wave at the input-port for a given wavelength of 1.55 μm. The spectral response of TE and TM wave of the MRR is shown in Fig.3. It is concluded from the simulation results that a good coupling effect of both TE and TM waves can be obtained.

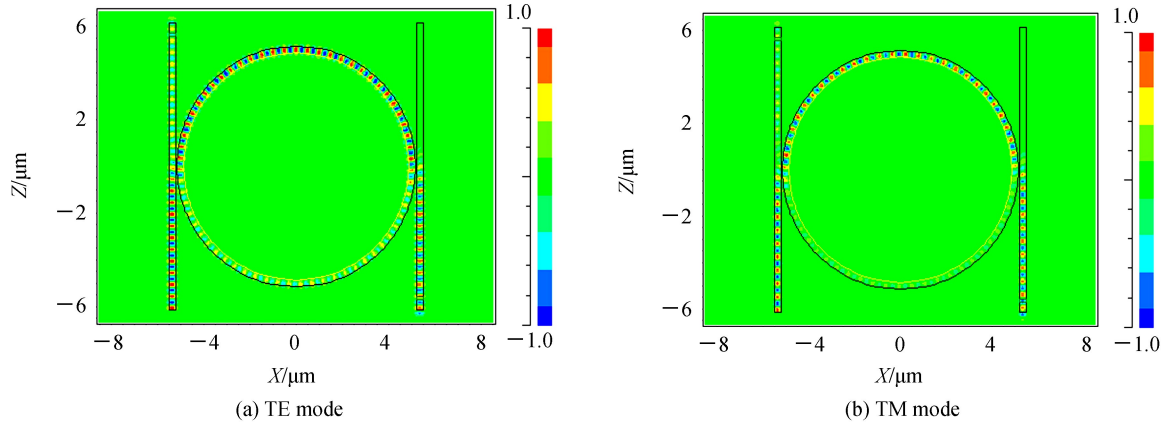

Fig.3 Simulation results of electric field distribution for microring resonator

The simulated dispersion curves of the effective indices for both the quasi-TE mode and the quasi-TM mode have been shown in the early paper[13] using the full-vectorial finite-difference mode. The good

agreement between the simulated and the experimental results showed that when the slot was introduced, the effective refractive index of the quasi-TE mode significantly decreased while that of the quasi-TM mode was only slightly affected. This phenomenon proves that, for the quasi-TE mode, light is indeed concentrated in the low-index region because of the field discontinuity[13].

To study the property of slot waveguide designed in Fig. 1, the simulated refractive indices for both quasi-TE and quasi-TM modes of the slot waveguide are shown in Table 1, which have been verified by the experiments in Ref.[13]. The simulation is also based on the full-vectorial finite-difference mode.

Table 1 The value of n_{eff} and n_g for TE mode and TM mode

Mode	TE(1.91 μm)		TM(1.55 μm)	
Value	n_{eff}	n_g	n_{eff}	n_g
	1.56	2.12	1.76	3.24

With the increase of heating power in the coupling region, the silicon refractive index n increases so that the refractive index difference Δn between core (Si) and cladding (SiO_2) increases as well. The enhanced electric field inside the gap raises because of the increase of refractive index difference changes the energy in the gap. Table 1 gives the values of n_{eff} and the group index n_g. The change of refractive index difference Δn caused by thermo-optical effect is dependent on the change of the effective index of $\Delta n = (dn/dT)_{Si}\Delta T$, in which $(dn/dT)_{Si} = +1.84 \times 10^{-4} K^{-1}$ is the thermo-optical coefficient of silicon[14]. Accordingly, a temperature change of $\Delta T = 54.35K$ is needed to obtain a Δn change of 0.01. Heater power can be calculated by [15]

$$P = \Delta T k_{SiO2} L (w/t_{SiO2} + 0.88) \tag{13}$$

Where $k_{SiO2} = 1.4W(m \cdot K)^{-1}$ is the thermal conductivity of SiO_2 layer with the thickness of $t_{SiO2} = 1$ μm. The width of the heater is $w = 4$ μm. Therefore, the heater power of $P = 0.371$ mW is needed for $\Delta n = 2.03$, while $P = 0.742$ mW is needed for $\Delta n = 2.04$.

By using FDTD method, the coupling effect between the straight waveguide and microring is studied by injecting a continuous wave at the input-port for a given wavelength of 1550nm. The self-coupling coefficient t, energy factor K and inner circulation factor α are accordingly obtained. The values of t^2 and K^2 related to the different value of Δn are shown in Table 2.

Table 2 Values of t^2 and K^2 related to the different value of Δn, which is calculated by FDTD method

HEAT	0	0.371mW	0.742mW
Δn	2.02	2.03	2.04
t^2	0.522	0.505	0.485
K^2	0.478	0.495	0.515
α	0.97	0.98	0.99

Now a pulsed light with the given wavelength of 1 550 nm is injected into the input-port. Fig. 4 shows the monitor value of TM mode response for wavelength with the heat source of 0, 0.371 mW and 0.742 mW. For TM mode, with the heat power increasing, the central wavelength remains to be 1542.8nm, while the bandwidth of the MRR ($\Delta\lambda$) varies from 634.1 nm (with 0 power) to 635.6 nm (with 0.371 mW) and finally to 637.2 nm (with 0.742 mW). The bandwidth of the MRR ($\Delta\lambda$) can be tuned from 1.5 nm with 0.371 mW to 3.1 nm with 0.742 mW heat power with a fixed central wavelength of 1 542.8 nm.

Fig.5 shows the monitor value of TE mode response for wavelength when applying different heat source. From Fig. 5, with the heat power increasing, the central wavelength varies from 1 900.2 nm, to 1 905.8 nm and 1 906.6 nm. It indicates that the MRR has good polarization characteristics with a central wavelength of 1 542 nm for TE mode and that of 1 900 nm for TM mode. In addition, the bandwidth of the MRR ($\Delta\lambda$) varies from 1 257.2 nm (with 0 power) to 1 258.5 nm (with 0.371 mW) and finally to 1 259.7 nm (with 0.742 mW). Based on the thermo-optical modulation, for TE mode, the central wavelength of MRR can be adjusted from 1900 nm to 1 906.6 nm, and tunable range of its $\Delta\lambda$ is from 1.3 nm to 2.5 nm.

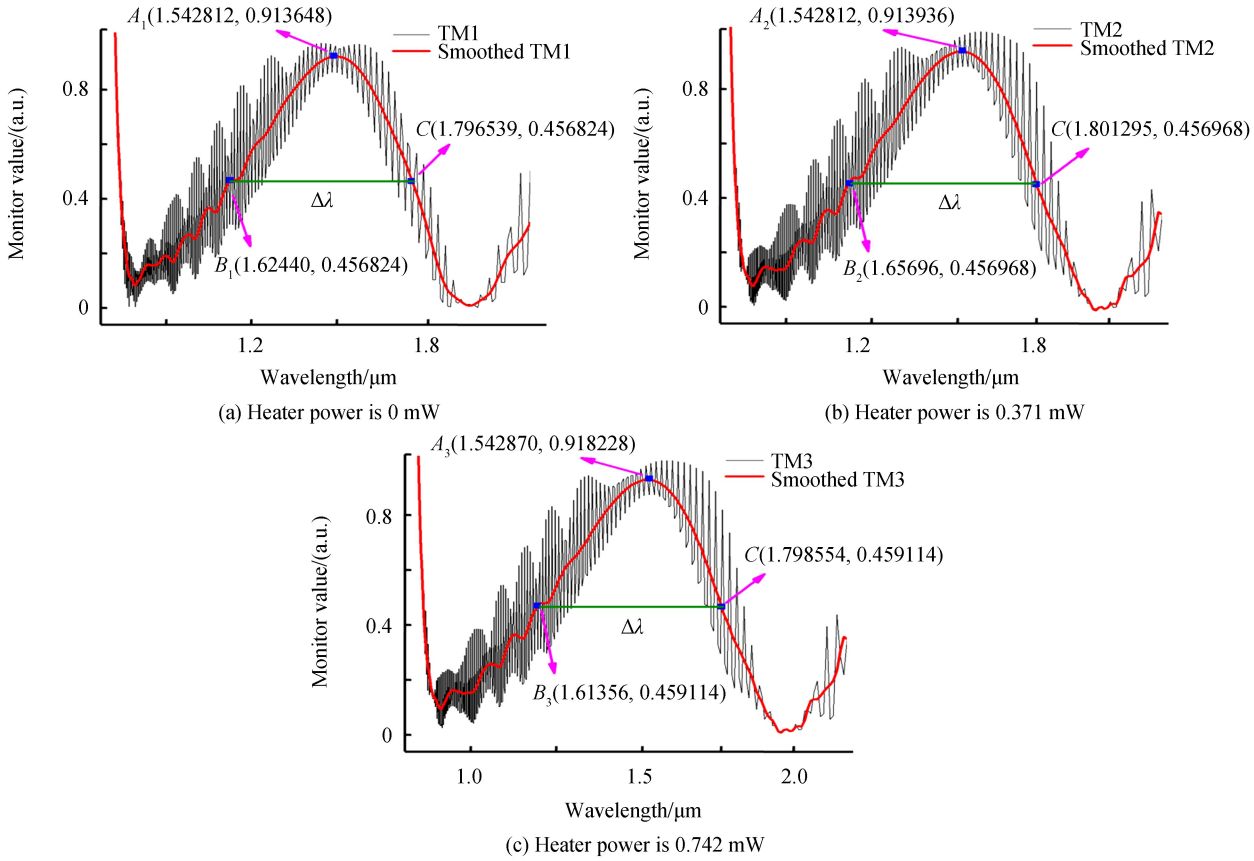

Fig.4 Monitor value of TM response for wavelength

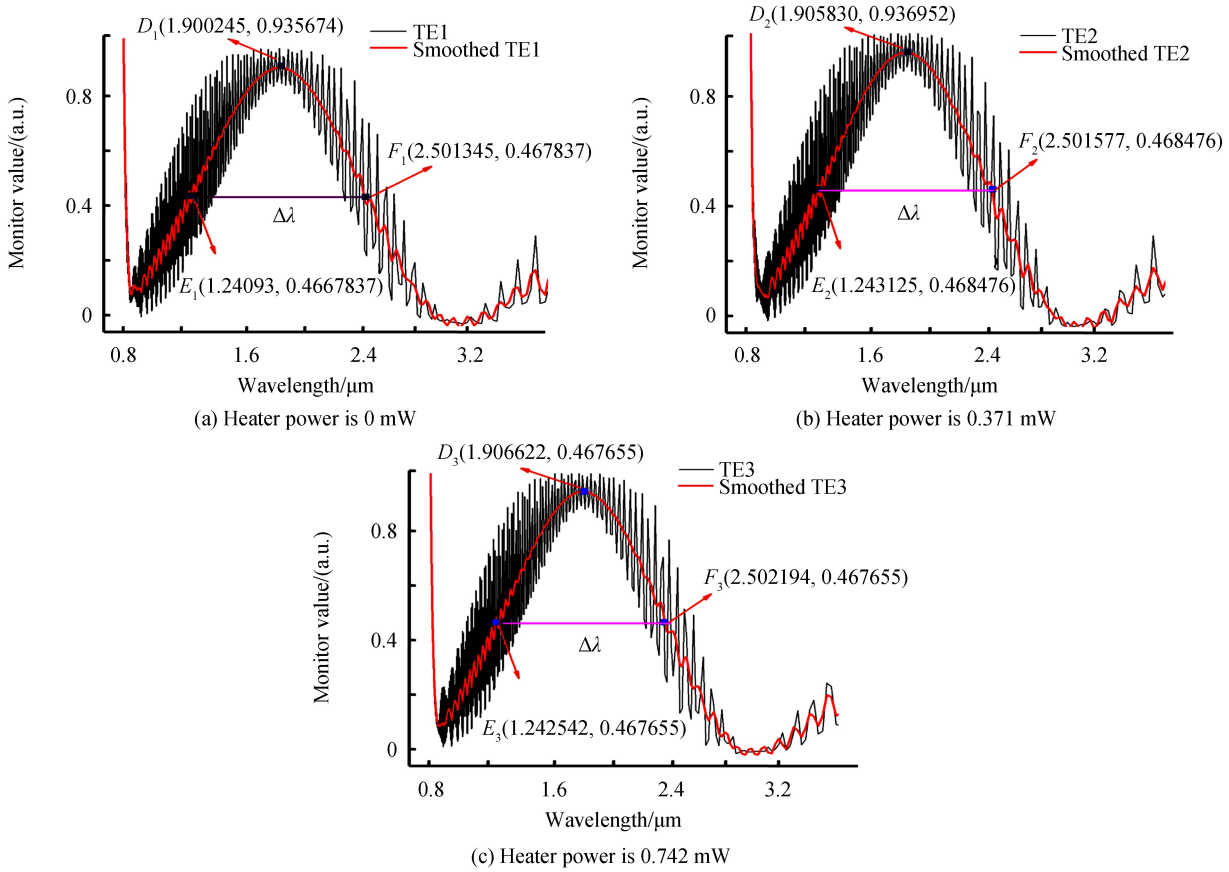

Fig.5 Monitor value of TE response for wavelength

3 Conclusion

An ultra-compact microring resonator on silicon-on-insulator with the size of 15 μm × 20 μm is proposed and numerical demonstrated. It indicated that the MRR is a polarized optical device with the central wavelength of 1 900 nm for TE mode and that of 1 543 nm for TM mode based on the characteristics of slot waveguides. By the thermo-optical modulating, the bandwidth of MRR can be tuned effectively. For TM mode, with the heat power increasing, the bandwidth of the MRR ($\Delta\lambda$) can be tuned from 1.5 nm with 0.371 mW to 3.1 nm with 0.742 mW heat power with a fixed central wavelength of 1 542.8 nm. In addition, for TE mode, the central wavelength of MRR can be adjusted from 1 900 nm to 1 906.6 nm, and tunable range of its $\Delta\lambda$ is from 1.3 nm to 2.5 nm. With further and deeply researches such as studying the effect of heater's temperature uniformity on the performance of device, how the responding speed of device is affected by that of heater's thermal effect and the accuracy limit of resonator, etc., the micro-device will be very promising for dynamic integrated optical signal processing.

References

[1] EHRLICHMAN Y, KHILO A, POPOVIC M A. Optimal design of a microring cavity optical modulator for efficient RF-to-optical conversion[J].*Optics Express*, 2018, **26**(3): 2462-2477.

[2] TAN Ying, WU Hao, DAI Dao-xin. Silicon-based hybrid (de) multiplexer for wavelength-/polarization-division-multiplexing[J].*Journal of Lightwave Technology*, 2018, **36**(11): 2051-2058.

[3] ONG J R, KUMAR R, MOOKHERJEA S. Silicon microring-based wavelength converter with integrated pump and signal suppression[J].*Optics Letters*, 2014, **39**(15): 4439-4441.

[4] VLASOV Y, GREEN W M J, XIA F. High-throughput silicon nanophotonic wavelength-insensitive switch for on-chip optical networks[J].*Nature Photonics*, 2008, **2**: 242-246.

[5] PAWLOWSKI E, TAKIGUCHI K, OKUNO M, *et al*. Variable bandwidth and tunable centre frequency filter using transversal-form programmable optical filter[J]. *Electronics Letters*, 1996, **32**: 113-114.

[6] CHANG M, LEE M, WU M. Variable bandwidth of dynamic add-drop filters based on coupling-controlled microdisk resonators[J].*Optics Letters*, 2006, **31**: 2444-2446.

[7] DING Yun-hong, PU Min-hao, LIU Liu, *et al*. Bandwidth and wavelength-tunable optical bandpass filter based on silicon microring-MZI structure[J].*Optics Express*, 2011, **19**: 6462-6470.

[8] CHEN Long, SHERWOOD-DROZ N, LIPISON M. Compact bandwidth-tunable microring reasonaters[J]. *Optics Letters*, 2007, **21** (22): 3361-3363.

[9] HUANG Meng-hao, LI Si-min, WU Lu-gang, *et al*. A bandwidth-tunable flat-top optical filter based on a single reflective-type microring resonator[C]. 2015 14th International Conference on Optical Communications and Networks (IC0CN), 2015:15399298.

[10] ALMEIDA V R, XU Q, BARRIOS C A, *et al*. Guiding and confining light in void nanostructure[J].*Optics Letters*, 2004, **29**: 1209-1211.

[11] YARIV A. Universal relations for coupling of optical power between microresonators and dielectric waveguides[J]. *Electronics Letters*, 2000, **36**: 321-322.

[12] HESAI L, DAI Tao-xin.Micro-nano photonic integrated[M]. Science Press, 2010.

[13] XU Qian-fan, ALMEIDA V R, PANEPUCCI R R, *et al*. Experimental demonstration of guiding and confining light in nanometer-size low-refractive-index material[J]. *Optics Letters*, 2004, **29**(14): 1626-1628.

[14] COCORULLO G, RENDINA I. Thermo-optical modulation at 1.5 mu m in silicon etalon[J].*Electronics Letters*, 1992, **28**: 83-85.

[15] HIDA Y, ONOSE H, IMAMURA S. Polymer waveguide thermo optic switch with low electric power consumption at 1.3 μm[J]. *IEEE Photonics Technology Letters*, 1993, **5**(7): 782-784.

引用格式: DONG Wen, ZOU Yu, DU Ying, *et al*. Ultra-compact Bandwidth-tunable Microring Resonator[J]. *Acta Photonica Sinica*, 2018, **47**(8):0823001

董文,邹雨,杜颖,等.超小型带宽可调谐微环谐振腔[J].光子学报,2018,**47**(8):0823001